

Gene and Polymorphism Content of the HLA Complex and Its Relevance to Transplantation

*" HLA Kompleks Gen ve Polimorfizmlerinin
Transplantasyon ile İlişkisi "*

Mehmet Tefvik DORAK, MD PhD

*School of Life Sciences, Pharmacy & Chemistry
Kingston University London*

Istanbul, 29 March 2024



Outline

**HLA Complex and Its Unique Features
Gene and Polymorphism Update (2024)**

**Transplantation-related Gene Content
(Classical HLA genes; HLA-DP; HLA-F; HLA-G; MICA/MICB)**

History / Nostalgia

Histocompatibility Studies & H-2

Naming of HLA ("Antigens")

Solid Organ Transplantation

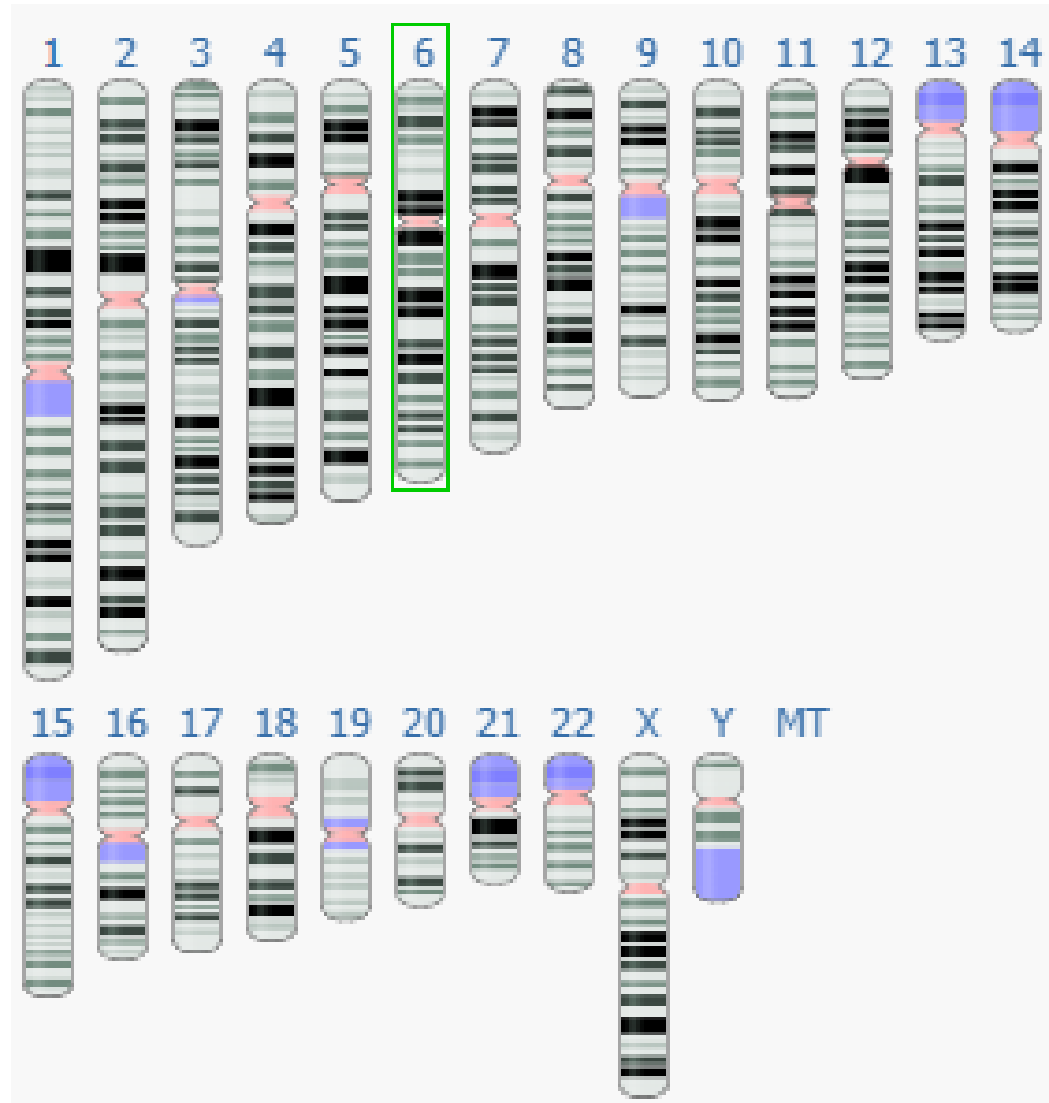
Bone Marrow Transplantation / HSCT

Immunosuppressives

.....

BMT 1992 Paper

Chromosome 6



MHC

TABLE 2 Sequenced cell lines and assembled haplotypes—summary of sequencing and assembly statistics

Cell line	MHC class II type	MHC assembly (bp)	MHC class II (bp)	MHC read depth			GenBank ID
				Nanopore	Illumina (WG)	PacBio (WG)	
APD	DR3	4.928.029	149.477	31,65	16,26	11,10	OK649231
DBB	DR4	5.048.108	260.711	20,03	12,91	11,50	OK649232
MANN	DR4	5.025.203	259.962	27,62	18,19	11,10	OK649234
SSTO	DR4	5.045.615	258.762	22,43	15,04	9,61	OK649236
KAS116	DR1	4.907.004	155.951	85,87	NA	11,10	OK649233
QBL	DR3	4.904.614	149.416	17,81	12,86	8,95	OK649235
COX	DR3	4.795.265	153.371	NA	NA	NA	GL000251.2
PGF	DR2	4.873.646	169.898	NA	NA	NA	chr6:28510120–33.480.575 (GRCh38)

Complete sequences of six major histocompatibility complex haplotypes, including all the major MHC class II structures

Torsten Houwaart¹ | Stephan Scholz¹ | Nicholas R. Pollock^{2,3} | William H. Palmer^{2,3} | Katherine M. Kichula^{2,3} | Daniel Strelow¹ | Duyen B. Le¹ | Dana Belick¹ | Lisanna Hülse¹ | Tobias Lautwein⁴ | Thorsten Wachtmeister⁴ | Tassilo E. Wollenweber⁴ | Birgit Henrich¹ | Karl Köhrer⁴ | Peter Parham⁵ | Lisbeth A. Guethlein⁵ | Paul J. Norman^{2,3} | Alexander T. Dilthey¹

MHC

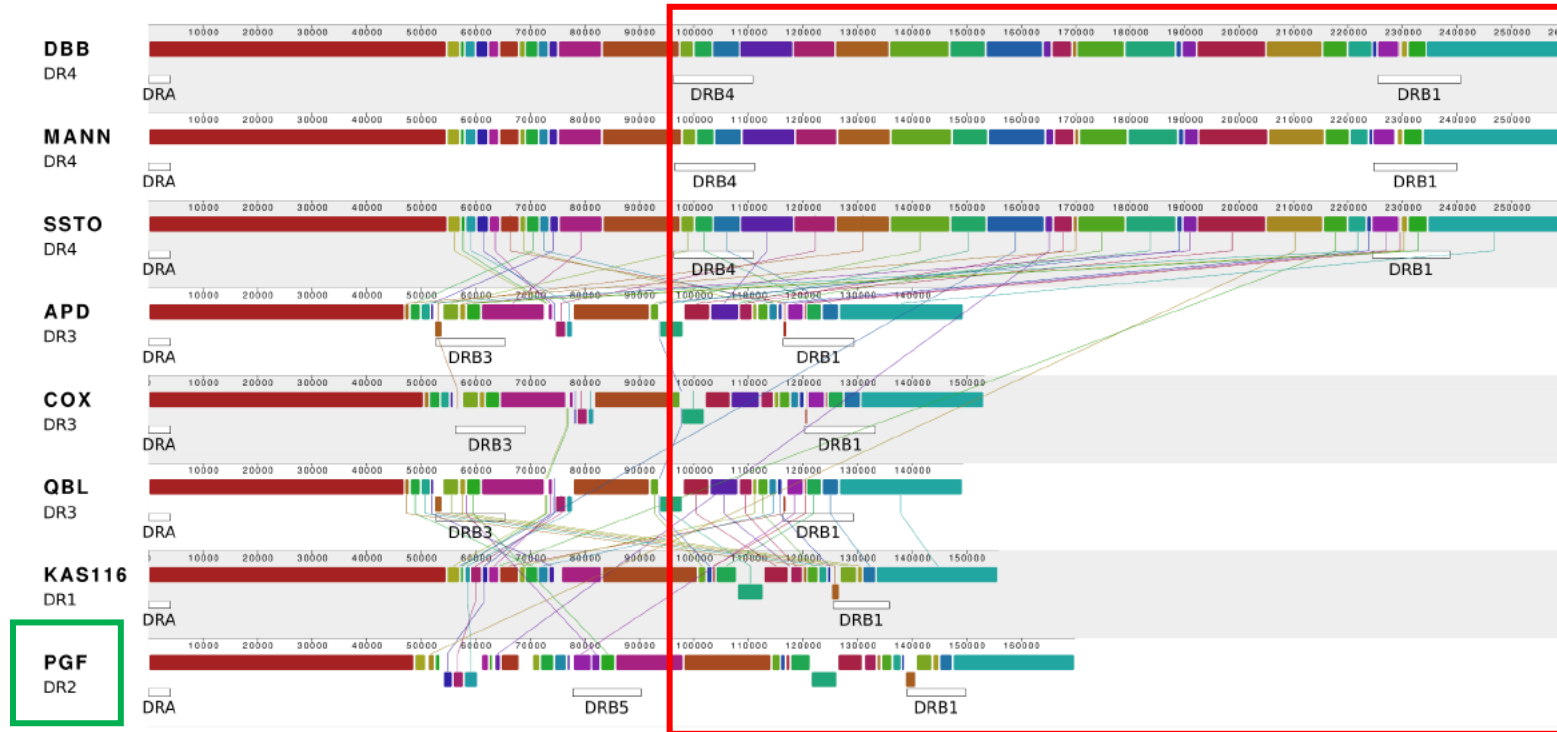


FIGURE 3 Multiple-sequence alignment visualization of *MHC class II* haplotype structures. Shown is a comparison of the eight completed *MHC class II* region sequences. Colors represent respective sequence similarity across haplotypes. Segments drawn underneath the respective plots represent inversions. The plot was created using Mauve⁵³ with parameter “seed weight” set to 22. Vertical lines connecting horizontally aligned homologous regions were edited for clarity.

Complete sequences of six major histocompatibility complex haplotypes, including all the major MHC class II structures

Torsten Houwaart¹ | Stephan Scholz¹ | Nicholas R. Pollock^{2,3} | William H. Palmer^{2,3} | Katherine M. Kichula^{2,3} | Daniel Strelow¹ | Duyen B. Le¹ | Dana Belick¹ | Lisanna Hülse¹ | Tobias Lautwein⁴ | Thorsten Wachtmeister⁴ | Tassilo E. Wollenweber⁴ | Birgit Henrich¹ | Karl Köhrer⁴ | Peter Parham⁵ | Lisbeth A. Guethlein⁵ | Paul J. Norman^{2,3} | Alexander T. Dilthey¹

MHC

	A	B	C	D	E
1	hgnc_id	symbol	name	locus_group	locus_type
14	HGNC:35418	GTF2H2C_2	GTF2H2 family member C, copy 2	protein-coding gene	gene with protein product
15	HGNC:4950	HLA-DRB2	major histocompatibility complex, class II, DR	pseudogene	pseudogene
16	HGNC:4951	HLA-DRB3	major histocompatibility complex, class II, DR	protein-coding gene	gene with protein product
17	HGNC:4952	HLA-DRB4	major histocompatibility complex, class II, DR	protein-coding gene	gene with protein product
18	HGNC:4955	HLA-DRB7	major histocompatibility complex, class II, DR	pseudogene	pseudogene
19	HGNC:4956	HLA-DRB8	major histocompatibility complex, class II, DR	pseudogene	pseudogene
20	HGNC:5923	IGLV5-39	immunoglobulin lambda variable 5-39	other	immunoglobulin gene
21	HGNC:6330	KIR2DL2	killer cell immunoglobulin like receptor, two Ig	protein-coding gene	gene with protein product
22	HGNC:16345	KIR2DL5A	killer cell immunoglobulin like receptor, two Ig	protein-coding gene	gene with protein product
23	HGNC:16346	KIR2DL5B	killer cell immunoglobulin like receptor, two Ig	protein-coding gene	gene with protein product
24	HGNC:6604	LILRA3	leukocyte immunoglobulin like receptor A3	protein-coding gene	gene with protein product
25	HGNC:42096	MTND1P13	MT-ND1 pseudogene 13	pseudogene	pseudogene
26	HGNC:27538	OR8U8	olfactory receptor family 8 subfamily U member	protein-coding gene	gene with protein product
27	HGNC:29166	OR8U9	olfactory receptor family 8 subfamily U member	protein-coding gene	gene with protein product
28	HGNC:31940	OR9G9	olfactory receptor family 9 subfamily G member	protein-coding gene	gene with protein product
29	HGNC:16376	FAM8A5P	family with sequence similarity 8 member A5, pseudogene	pseudogene	pseudogene
30	HGNC:34393	PRAMEF22	PRAME family member 22	other	unknown
31	HGNC:33447	PRKRAP1	protein activator of interferon induced protein	pseudogene	pseudogene
32	HGNC:43788	PRSS3P2	PRSS3 pseudogene 2	pseudogene	pseudogene
33	HGNC:48421	RNU1-79P	RNA, U1 small nuclear 79, pseudogene	pseudogene	pseudogene

HGNC



Gene data ▾



Tools ▾



Downloads ▾



VGNC ▾

Contact us ▾

Statistics & download files ?

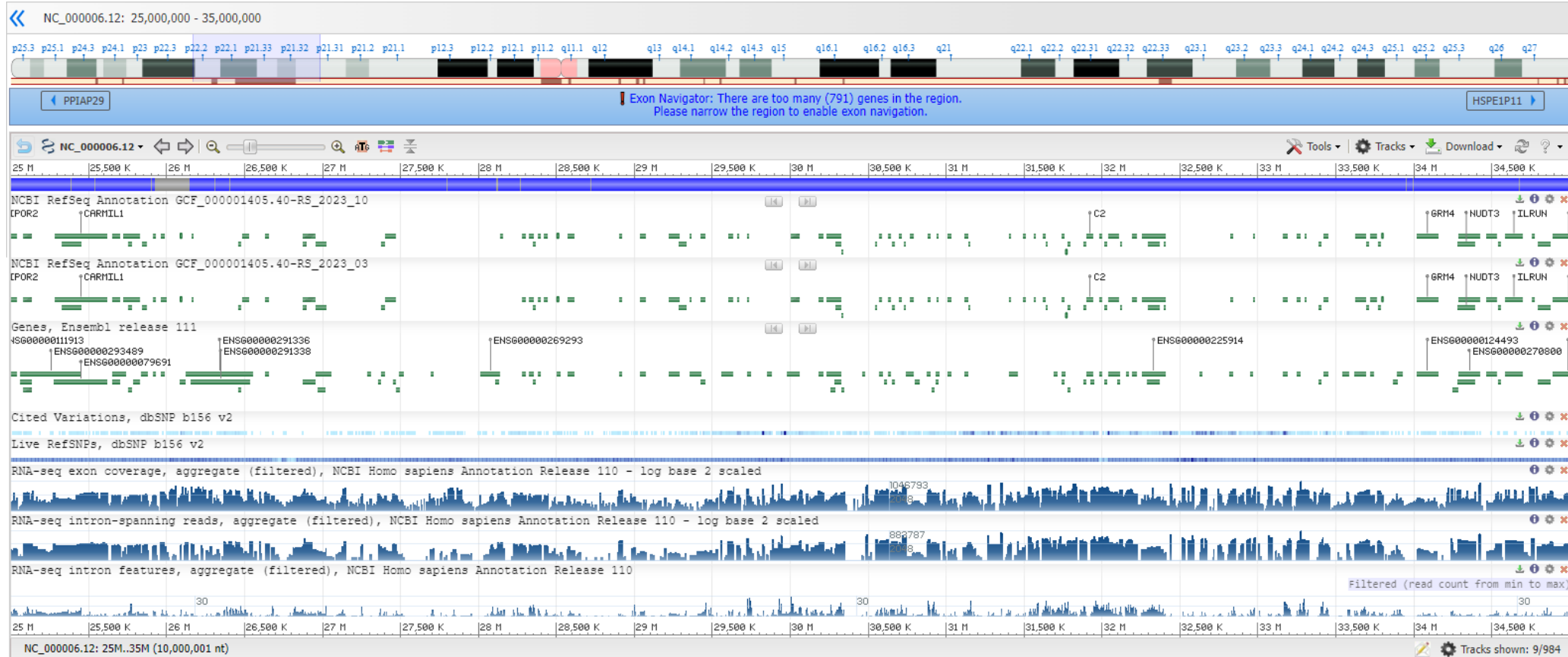
xMHC

Genome Data Viewer

Homo sapiens
(human)

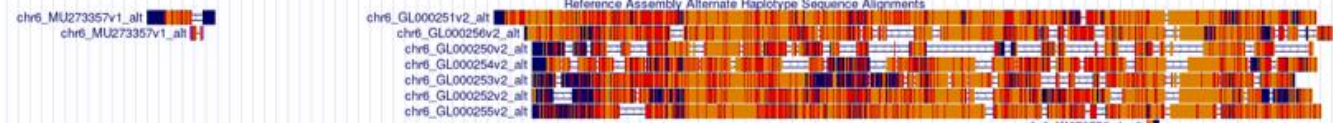
Assembly: GRCh38.p14 (GCF_000001405.40)

Chr 6 (NC_000006.12)





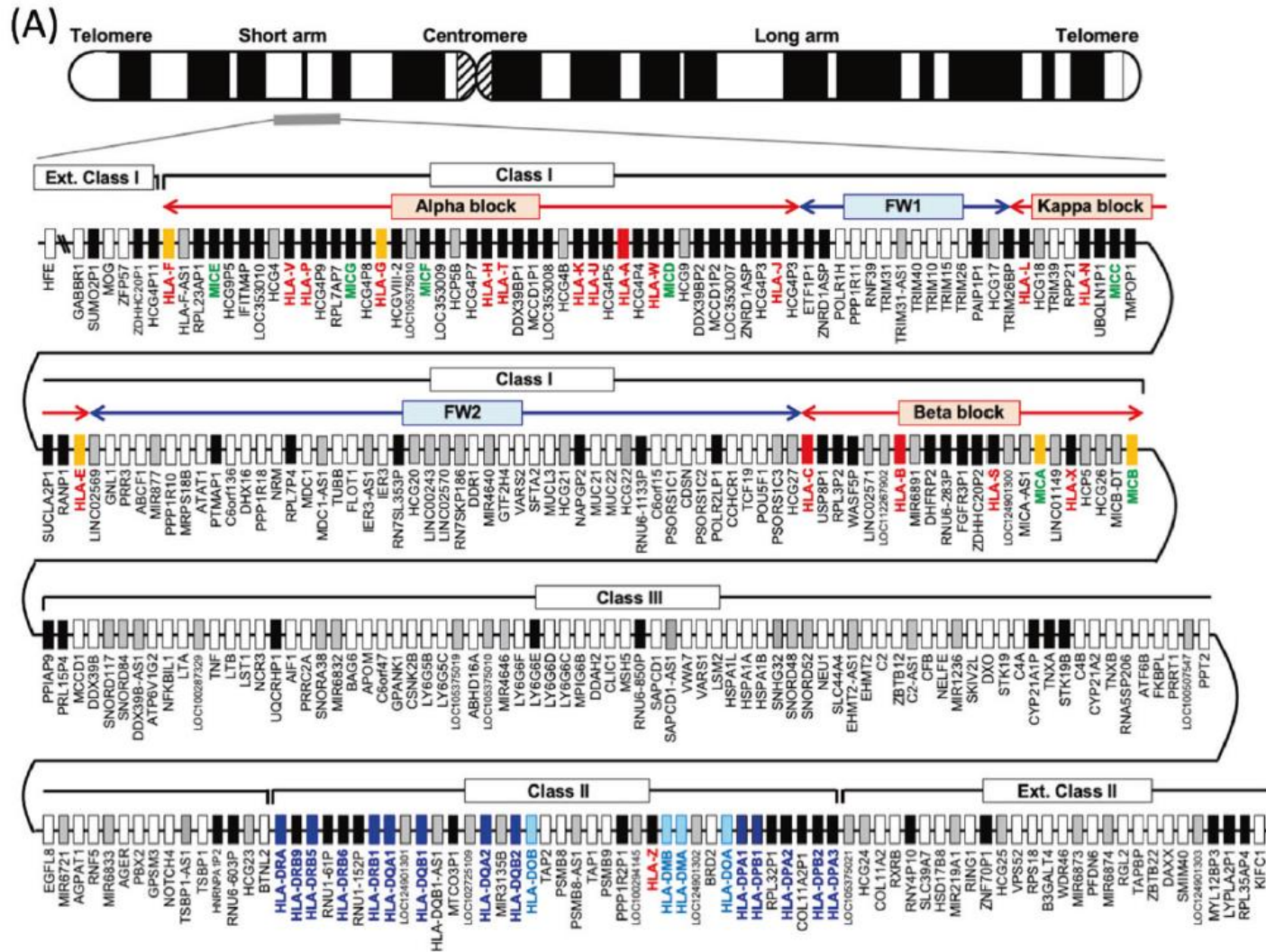
Scale chr6: 25,500,000 26,000,000 26,500,000 27,000,000 27,500,000 5 Mb hg38 28,000,000 28,500,000 29,000,000 29,500,000 30,000,000 30,500,000 31,000,000 31,500,000 32,000,000 32,500,000 33,000,000 33,500,000 34,000,000 34,500,000



GENCODE V44 (1451 items filtered out)

ENSG00000296633	SCGN H1-1 BTN2A1 LARRPM ZNF184 H1-5 PGBD1 LINC01623 OR14J1 MOG RNF39 HLA-E DDR1 HLA-C LTA C2 BTNL2 TAP2 RXRB BAK1 GRM4 SPDEF
RN7SL334P	H2AC1 H1-2 BTN1A1 RNU2-62P1 H2BC13 NKAPL HCG141 OR5V1 HLA-F TRIM10 GNL1 SFTA2 HLA-B GLIC1 C4B RNU1-61P1 BRD2 KIFC1 MLN1 HMGA1 SNRPC
ENSG00000229313	H2BC1 HFE HCG11 H2BC11 H2AC13 ZSCAN31 TRIM27 OR12D3 HLA-G HCG17-4 NRM C6orf15 Y_RNA NEU1 TSBP1 PSMB8 RING1 ITR3 MIR6835 BLTP3A
ENSG00000223623	SLC17A4 H1-6 HMGNA4 H2AC11 H3C10 ZSCAN3 RNU6-939P OR12D2 HOP5B HLA-LH MDC1 CDSN MICB C2-AS1 HLA-DRA HLA-DRB1 TAP1 HCG25 UCC2 SMIM29 Y_RNA
ENSG00000285801	CARMIL1 H3C9 H2BC12 H2AC14 ZSCAN12 LINC01556 OR12D1 HLA-A RPP21 TUBB TCF19 TNF CFB HLA-DRB5 HLA-DOA1 PHF1 MIR1591 RPS10 TAF11
RNU6-987P	Y_RNA1 SLC17A3 H3C1 H3C6 GUSBP2 ZNF391 H4C11 ZSCAN23 RNU2L471P OR11A1 H HCG9 LINC02569 VARS2 Y_RNA1 VYAT7 PPT2 HLA-DOA2 HCG24 MIR3934 NUDT3 RNY3P15
ENSG00000286933	RNU6-502P SLC17A2 H1-3 H3C3 ENSG00000272468 H4C12 ZSCAN23 GPX6 ZNF311 OR2H1 POLR1H PRR3 MUC2 MICA LSM2 RNF5 MIR3135B1 VPS52 IPK3 PACSINI ILRUN
ENSG00000290217	H4C1 ENSG00000272312 RNU6-471P U3 GPX5 OR2W1 MAS1L TRIM31 MIR5771 HCG32 DDX39B SKIC2 HLA-DRB1 COL11A2 MIR12751 RN7SL200P
ENSG00000272558	H4C3 ENSG00000290032 H2AC15 U3 SCAND3 OR2B3 OR21P TRIM40 ATAT1 CCHCR1 LTB D XO HLA-DOA1 RNY4P10 HCG51 ENSG00000288879 ANKSI1A
ENSG00000272810	TRIM38 BTN3A3 H2AC12 H2BC15 ZSCAN9 OR2W1-AS1 OR2J3 GABBR1 TRIM39 FLOT1 LINC02571 AIF1 TNXB HLA-DOB2 RPS18 ENSG0000022339 H
ENSG00000272810	LINC02980 MIR3143 H2AC16 LINC00533 OR2J3 GABBR1 TRIM39 FLOT1 LINC02571 AIF1 TNXB HLA-DOB2 RPS18 ENSG0000022339 H
ENSG00000272810	H3C2 PRSS16 H4C13 ENSG00000225173 LINC02829 TRIM31-AS1 PPP1R10 PSORS1C3 PRR2A ATF6B PSMB9 PFDN6
ENSG00000272810	H4C2 POM121L2 H3C12 ENSG00000244349 LINC01015 TRIM39-RPP21 Y_RNA MIR6891 MSH5 PRRT1 HLA-DMB RGL2
H2AC4	H2AC17 H2BC17 ENSG00000271755 H2AC17 ZBED9-AS1 OR2J1 OR2H2 TRIM15 C6orf136 POU5F1 LST1 STK19 HLA-DOB1 SLC39A7 ENSG00000248993 DAXX
H2BC3	H3C3 ENSG00000285849 H2BC17 ENSG00000284656 Y_RNA PPP1R18 RNU6-289P VARS1 AGER ENSG00000248993 DAXX
ENSG00000291336	ENSG00000285703 H OR2B6 ENSG00000290478 ENSG00000278104 OR2J2 ENSG00000290574 MDC1-AS1 LINC01149 EHMT2 HLA-DOB1-AS1 HSD17B8
H2BC4	H2AC6 ENSG00000287252 ZSCAN26 ENSG00000289203 ENSG00000286301 GTF2H4 SNORD171 C4A-AS1 ENSG00000250264 MIR6873
ENSG00000291338	ZSCAN16-AS1 OR2B8P ENSG00000272236 ENSG00000272540 ATP6V1G2 PPT2-EGFL8 ENSG00000289047 SYNGAP1
ENSG00000289117	H2BC5 ENSG00000272009 ENSG00000290870 H LINC00243 H SNORA38 AGPAT1 ENSG00000291111
ENSG00000283064	H2BC6 ENSG00000291088 ENSG00000275856 LINC02570 BAG6 MIR6721 ENSG00000288751
ENSG00000282988	H4C4 ENSG00000290891 ENSG00000278773 RN7SKP186 APOM MIR6833 MIR219A1
ENSG00000282988	H3C4 ENSG00000252228 ENSG00000280909 DDR1-DT1 C6orf47 PBX2 ENSG00000272217
H2AC7	ZKSCAN8 ENSG00000261839 ENSG00000280128 MIR4640 C6orf47-AS1 GPM3 ENSG00000289975
H2BC7	ZKSCAN8P1 ENSG00000280107 ENSG00000288473 GPANK1 NOTCH4 B3GALT4
H4C5	ENSG00000280107 ENSG00000288473 MUCL3 Y_RNA RNU6-603P MIR6834
H2BC8	ZKSCAN4 ENSG00000276302 HCG21 CSNK2B ENSG00000232080 ZBTB22
H2AC8	ENSG00000289467 ENSG00000275011 ABHD16A ENSG00000289100
H4C6	ENSG00000290051 ENSG00000271821 MIR4646 ENSG00000285064
H3C7	ENSG00000287804 ENSG00000288813 LY6GEF ENSG00000289100
H2BC9	ENSG00000286819 ENSG00000288817 Y_RNA ENSG00000285064
H3C8	ENSG00000287279 ENSG00000288817 Y_RNA ENSG00000285064
ENSG00000290789	H2BC10 H4C8 ATP6V1G2-DDX39B ENSG00000289406
ENSG00000289447	ENSG00000289375 ENSG00000291302 ENSG00000289282
ENSG00000287050	BTN3A2 BTN2A2 BTN3A1 ENSG00000263020
ENSG00000290055	RNU6-502P LINC00204422
ENSG00000284407	ENSG00000284407 LY6GEF
ENSG00000275846	ENSG00000275846 LY6GEF
ENSG00000285571	ENSG00000285571 MPJ66
ENSG00000261584	ENSG00000261584 DDH2
	MSH5-SAPCD1
	RNU6-859P
	SAPCD1
	SAPCD1-AS1
	HSPA1L
	HSPA1A
	ENSG00000289637
	ENSG00000289829
	LY6G
	ENSG00000285565
	SNORD48
	SNORD52
	EHMT2-AS1
	ENSG00000244255
	ENSG00000290788
	ENSG00000284829 H
	ENSG00000286974
	ENSG00000285085
	ENSG00000273333

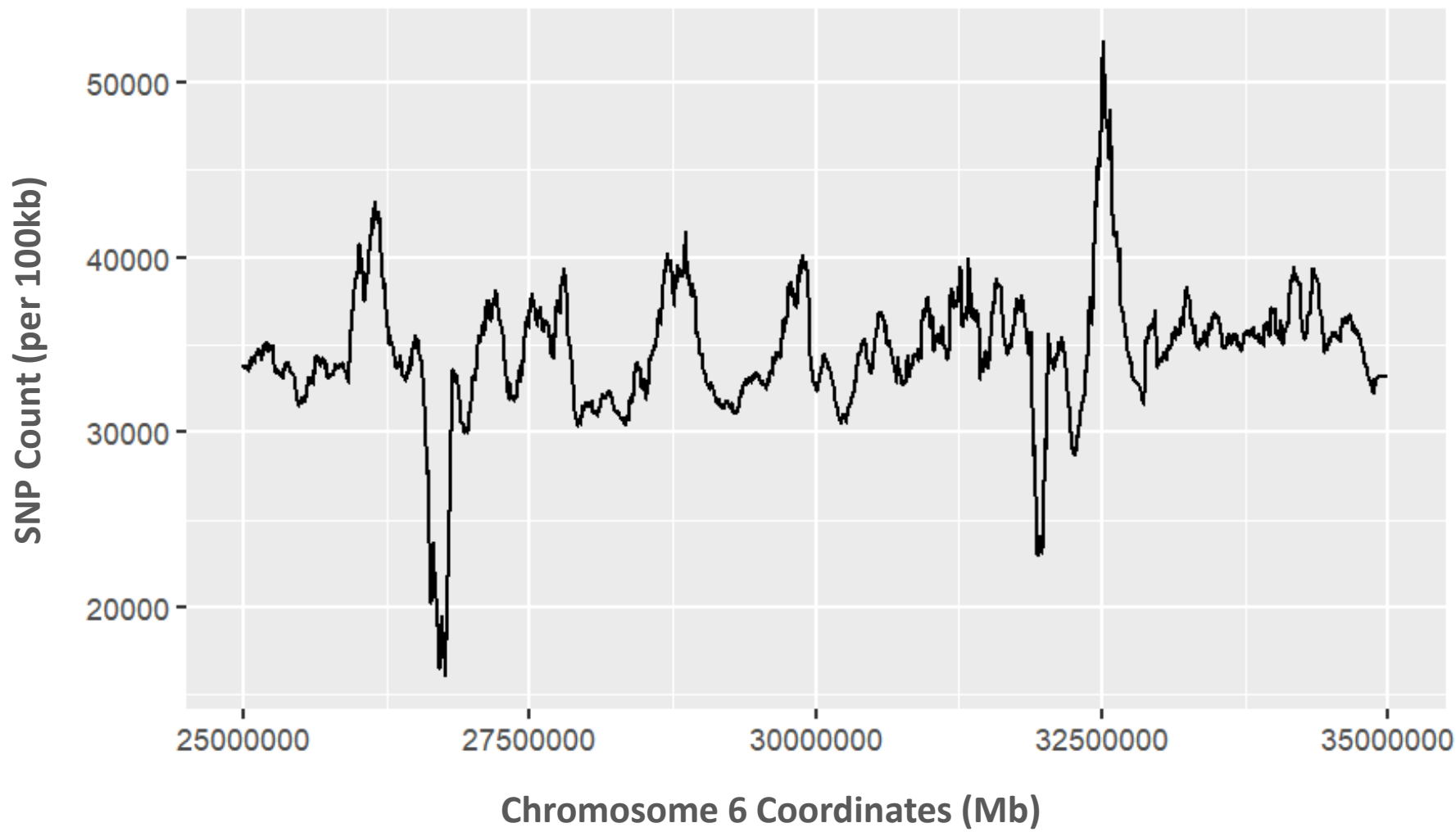
xMHC



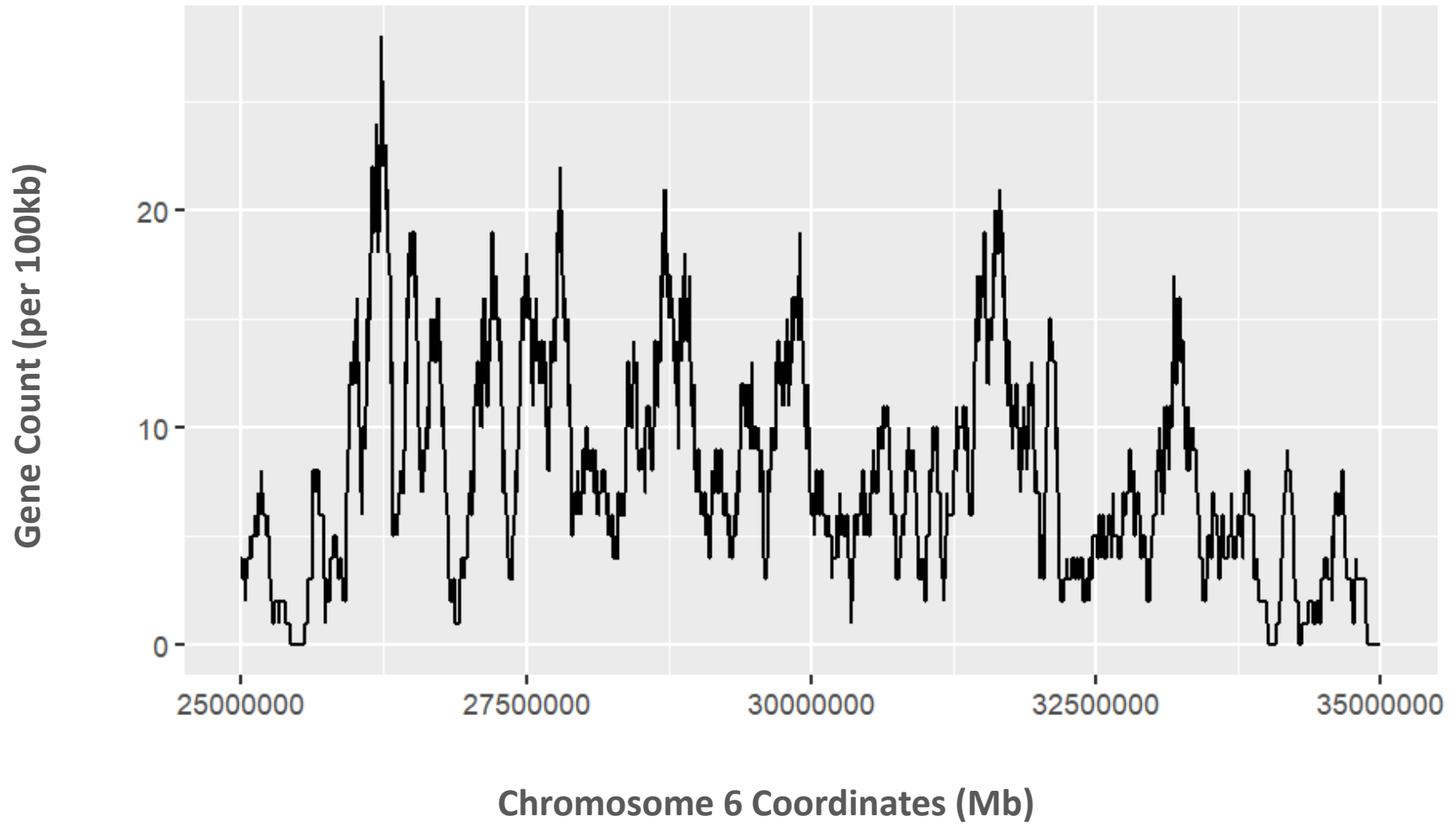
Human leukocyte antigen super-locus: nexus of genomic supergenes, SNPs, indels, transcripts, and haplotypes

Jerzy K. Kulski¹, Shingo Suzuki¹ and Takashi Shiina¹

SNP Density



Gene Density



xMHC: Unique Features

Genome (3.2Gb)	xHLA Region (25.7 to 33.4Mb)	Comparison
Total No of Genes 60155	Total No of Genes 674	...
Protein-coding genes 19881	Protein-coding genes 453	32.66 vs 67.21% <i>P</i> <0.0001
Non-coding RNA Genes 25411	Non-coding RNA Genes 54	42.63 vs 8.01% <i>P</i> <0.0001
Long non-coding RNA genes 15877	Long non-coding RNA genes 13	1.93 vs 26.39% <i>P</i> <0.0001
Small non-coding RNA genes 9534	Small non-coding RNA genes 7	1.04 vs 15.85% <i>P</i> <0.0001
Pseudogenes 14467	Pseudogenes 172	24.03 vs 25.52% <i>P</i> = 0.37

xHLA makes up 0.24% of the genome, but contains 0.40% of all SNPs in the human genome

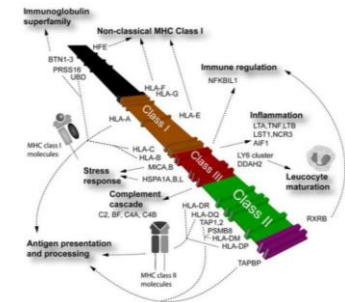
A systematic analysis of the gene and variation content of the extended HLA region

Ertan KANBUR, Mustafa DOGAN, Mehmet Tevfik DORAK

Presented at EFI 2017

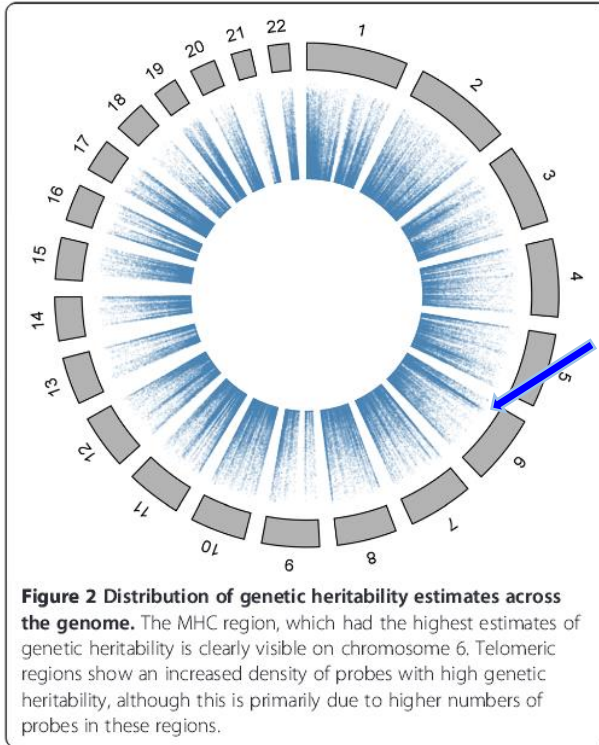
xMHC: Unique Features

- Most gene dense
- Extremely polymorphic
- Paralog regions and genes
- CNV and structural variation
- Very high linkage disequilibrium over very long-range resulting from conserved extended haplotypes (CEH)
- Greatest trans-eQTL density
- Highest genetic heritability estimates of DNA heritability
- Very strong selective coefficients
- Extreme geographical, racial and ethnic differential in allele frequencies
- So many lineages and groupings of alleles & haplotypes
- So many functional dimorphisms or supertypes with no single corresponding SNPs



xMHC: Unique Features

Heritability of DNA methylation



McRae et al. *Genome Biology* 2014, 15:R73
<http://genomebiology.com/2014/15/5/R73>



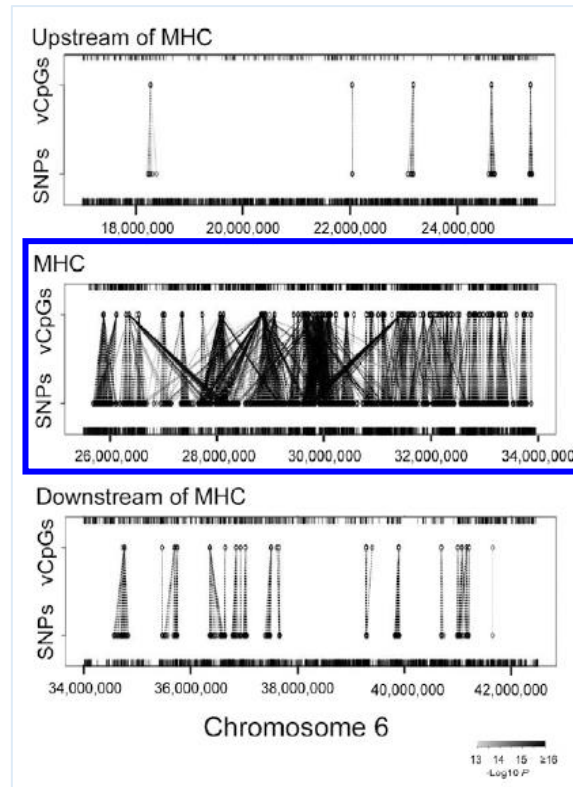
RESEARCH

Open Access

Contribution of genetic variation to transgenerational inheritance of DNA methylation

Allan F McRae^{1,2*}, Joseph E Powell^{1,2}, Anjali K Henders³, Lisa Bowdler³, Gibran Hemani^{1,2}, Sonia Shah^{1,2}, Jodie N Painter³, Nicholas G Martin³, Peter M Visscher^{1,2*} and Grant W Montgomery^{1*}

meQTL density



(E) Associations between CpG sites and SNPs upstream of (top panel), within (middle panel), or downstream of (bottom panel) the major histocompatibility complex (MHC) region. Each dashed line represents a significant association, and the shades of black indicate significance of the associations.

GeMes, Clusters of DNA Methylation under Genetic Control, Can Inform Genetic and Epigenetic Analysis of Disease

Yun Liu,^{1,2,9*} Xin Li,^{1,2,9*} Martin J. Aryee,^{1,3} Tomas J. Ekström,^{4,5} Leonid Padyukov,^{4,6} Lars Klareskog,^{4,6} Amy Vandiver,^{1,2} Ann Zenobia Moore,⁷ Toshiko Tanaka,⁷ Luigi Ferrucci,⁷ M. Daniele Fallin,^{1,8,*} and Andrew P. Feingberg^{1,2,*}

trans-eQTL density

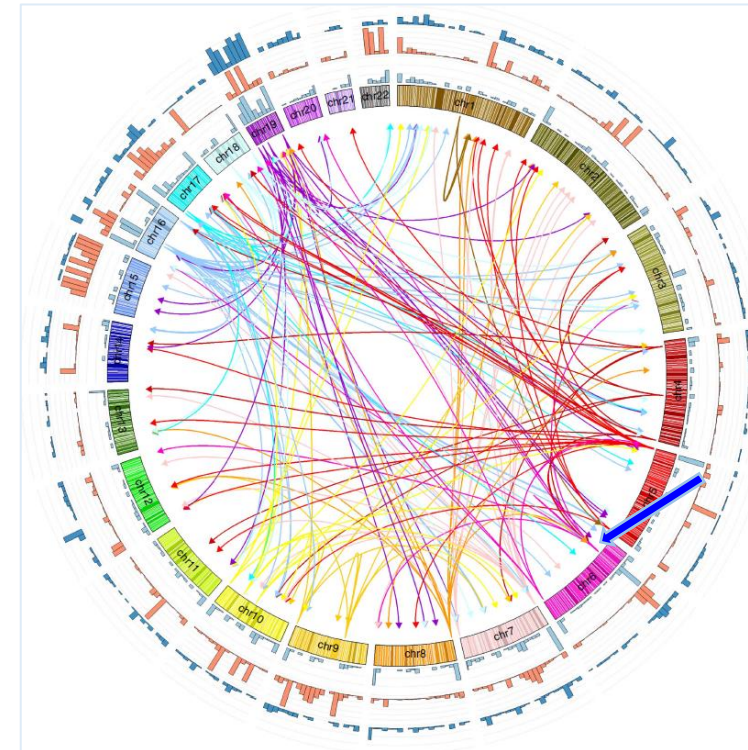


Figure 1 | Enrichment of features in regions harbouring SNPs involved in distal SNP-CpG associations. Outer histograms: number of SNPs involved in distal SNP-CpG associations (light blue), calculated in 7.5-Mb bins; number of piRNA sequences (orange); number of transcription factors (dark blue). Inner links: SNP regions associated with four or more CpG sites. Arrows are pointing from SNPs to the CpG sites they are associated with, and are coloured according to the chromosomes where the SNPs reside.

Long-range epigenetic regulation is conferred by genetic variation located at thousands of independent loci

Mathieu Lemire¹, Syed H.E. Zaidi¹, Maria Ban², Bing Ge³, Dylan Aissi^{4,5,6}, Marine Germain^{4,5,6}, Irfahan Kassam⁷, Mike Wang¹, Brent W. Zanke⁸, France Gagnon⁷, Pierre-Emmanuel Morange^{9,10,11}, David-Alexandre Tréguët^{4,5,6}, Philip S. Wells⁹, Stephen Sawcer², Steven Gallinger^{12,13}, Tomi Pastinen³ & Thomas J. Hudson^{1,14,15}

xMHC: Unique Features

trans-eQTLs

1	P Value	SNPName	SNPChr	SNPChrPos	ProbeName	ProbeChr	ProbeCenterChrPos	CisTrans	SNPType	Allele	OverallZScore
2	3.27167E-310	rs9268923	6	32432835	cg10154826	6	17601018	trans	C/T	T	61.2544774
3	3.27167E-310	rs2395185	6	32433167	cg10154826	6	17601018	trans	G/T	T	61.2544774
4	3.27167E-310	rs9268853	6	32429643	cg10154826	6	17601018	trans	T/C	C	61.1446653
5	3.27167E-310	rs477515	6	32569691	cg10154826	6	17601018	trans	G/A	A	58.2171575
6	3.27167E-310	rs4239020	17	80176641	cg07393940	7	158741793	trans	C/T	C	-55.4574242
7	3.27167E-310	rs12342831	9	33124872	cg20290983	6	43655494	trans	T/C	C	55.1041246
8	3.27167E-310	rs10813951	9	33128021	cg20290983	6	43655494	trans	A/G	G	55.0625727
9	3.27167E-310	rs12342831	9	33124872	cg04842962	6	43655513	trans	T/C	C	54.9486903
10	3.27167E-310	rs10813951	9	33128021	cg04842962	6	43655513	trans	A/G	G	54.9126278
11	3.27167E-310	rs3780486	9	33139453	cg20290983	6	43655494	trans	C/T	T	54.832052
12	3.27167E-310	rs3780486	9	33139453	cg04842962	6	43655513	trans	C/T	T	54.7699307
13	3.27167E-310	rs10813957	9	33153527	cg20290983	6	43655494	trans	G/T	T	54.7260295
14	3.27167E-310	rs10813957	9	33153527	cg04842962	6	43655513	trans	G/T	T	54.6814431
15	3.27167E-310	rs5756504	22	37467270	cg13737042	9	37806390	trans	C/T	T	-50.6708043
16	3.27167E-310	rs5756506	22	37467392	cg13737042	9	37806390	trans	G/C	C	-50.6605533
17	3.27167E-310	rs62103177	18	77624479	cg05926928	17	57297748	trans	G/A	A	49.4548764
18	3.27167E-310	rs8321	6	30032522	cg01620082	3	125678431	trans	A/C	C	-46.813694
19	3.27167E-310	rs2074977	19	3434028	cg08382705	11	45687343	trans	C/A	C	-46.6429193
20	3.27167E-310	rs8321	6	30032522	cg06606381	12	133084921	trans	A/C	C	-46.2606567

BIOS QTL browser

This web page accompanies the manuscripts titled 'Disease variants alter transcription factor levels and methylation of their binding sites', by Bonder & Luijk et al and 'Unbiased identification of regulatory modifiers of genetic risk factors', by Zhemakova et al, both have been submitted to Nature Genetics. For further questions, contact the corresponding author: lude@ludesign.nl

Download meQTL results

You can download the full cis- and trans-meQTL and eQTLs, detected at a false-discovery rate of 0.05:

[Cis-meQTLs](#)
[Cis-eQTLs](#)
[Trans-meQTLs](#)

Sex-differential in trait associations

NATURE GENETICS

ARTICLES

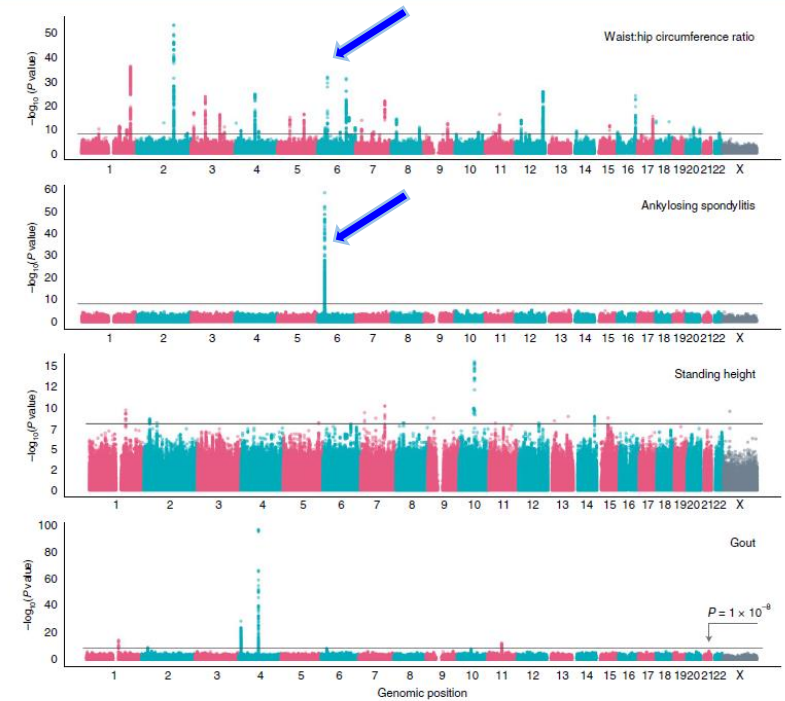
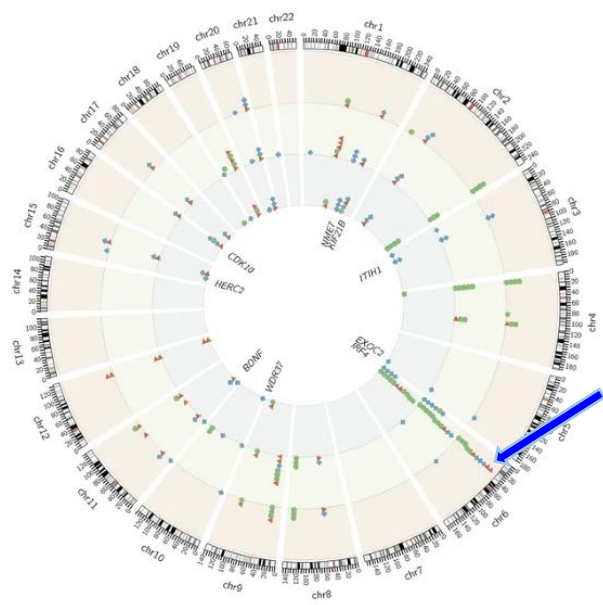


Fig. 3 | Manhattan plots for traits with most lead sdsSNPs. The x axis corresponds to the genomic position in the genome and the y axis to the $-\log_{10}(P \text{ value})$ of the two-sided Student's *t*-test (Methods), for which the null hypothesis is that there is no difference between the sexes. Each point corresponds to a genetic variant. Points that go above the statistical significance line at $-\log_{10}(P) = 1 \times 10^{-8}$ are considered to be sdsSNPs. Traits represented include: waist:hip circumference ratio, ankylosing spondylitis, standing height and gout.

Sex differences in genetic architecture in the UK Biobank

Elena Bernabeu¹, Oriol Canela-Xandri², Konrad Rawlik¹, Andrea Talenti¹, James Prendergast¹ and Albert Tenesa^{1,2}

xMHC: Unique Features



Overview of PheWAS associations in the genome after functional annotation. **a** This matrix shows the number of functional SNPs for their respective phenotype. **b** The *Circos plot* showing the PheWAS associations in different types of functional data. *Red triangles* represent the associations in the GWAS Catalog only, *green circles* represent GWAS Catalog associations replicated by PheWAS ($P < 0.05$), and *blue diamonds* represent new phenotype associations identified by PheWAS ($P < 4.6 \times 10^{-6}$ or $FDR < 0.1$)

including:

- Schizophrenia
- Alzheimer disease
- Parkinson disease
- Lung cancer
- Hodgkin lymphoma

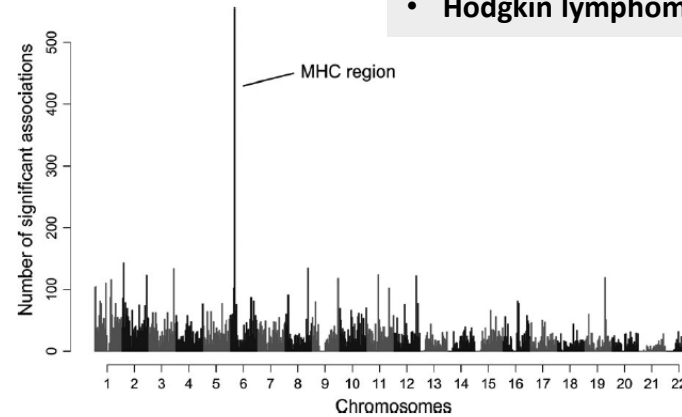


FIGURE 1 Number of significant GWAS associations along the genome. The chromosomal location of significant trait associations from GWAS ($N = 18,682$) is shown for all autosomes. Data from NHGRI GWAS catalog. Reproduced from "Lenz TL, Spirin V, Jordan DM, Sunyaev SR. Excess of Deleterious Mutations around HLA Genes Reveals Evolutionary Cost of Balancing Selection. *Mol Biol Evol* 2016;33(10):2555-64. <https://doi.org/10.1093/molbev/msw127>" by permission of Oxford University Press on behalf of the Society for Molecular Biology and Evolution

.... despite already showing the highest number of disease associations, the true extent of the involvement of the MHC region in disease genetics may not have been uncovered.

Zhao et al. *Genome Medicine* (2018) 10:7
DOI 10.1186/s13073-018-0513-x

Genome Medicine

RESEARCH Open Access

An integrative functional genomics framework for effective identification of novel regulatory variants in genome-phenome studies

Junfei Zhao^{1*}, Feixiong Cheng^{2,3†}, Peilin Jia¹, Nancy Cox^{4,5}, Joshua C. Denny^{5,6} and Zhongming Zhao^{1,2*}

*Correspondence: zhaof@broadinstitute.org

†Equal contributors: fcheng@broadinstitute.org

¹Broad Institute of MIT and Harvard, 77 Avenue Louis Pasteur, Cambridge, MA 02142, USA

²Department of Genetics, Harvard Medical School, 77 Avenue Louis Pasteur, Cambridge, MA 02142, USA

³Department of Biostatistics, Harvard Medical School, 77 Avenue Louis Pasteur, Cambridge, MA 02142, USA

⁴Department of Biostatistics, Harvard Medical School, 77 Avenue Louis Pasteur, Cambridge, MA 02142, USA

⁵Department of Biostatistics, Harvard Medical School, 77 Avenue Louis Pasteur, Cambridge, MA 02142, USA

⁶Department of Biostatistics, Harvard Medical School, 77 Avenue Louis Pasteur, Cambridge, MA 02142, USA

© The Author(s). 2018

Received: 9 March 2017 | Revised: 16 June 2017 | Accepted: 20 July 2017

DOI: 10.1111/jmi.12332

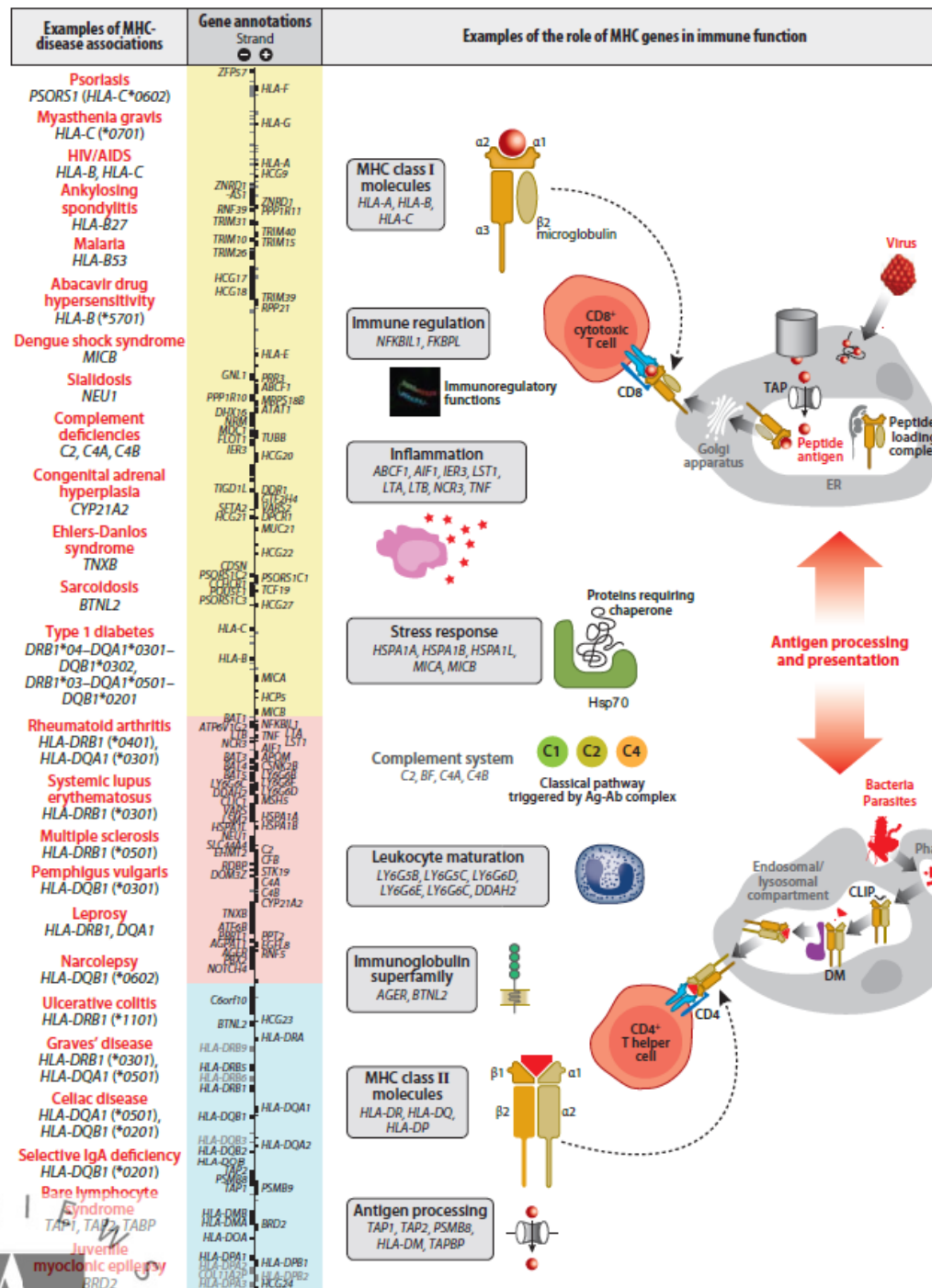
REVIEW

WILEY INTERNATIONAL JOURNAL OF IMMUNOGENETICS

What has GWAS done for HLA and disease associations?

A. E. Kennedy¹ | U. Ozbek^{2,3} | M. T. Dorak⁴

HLA

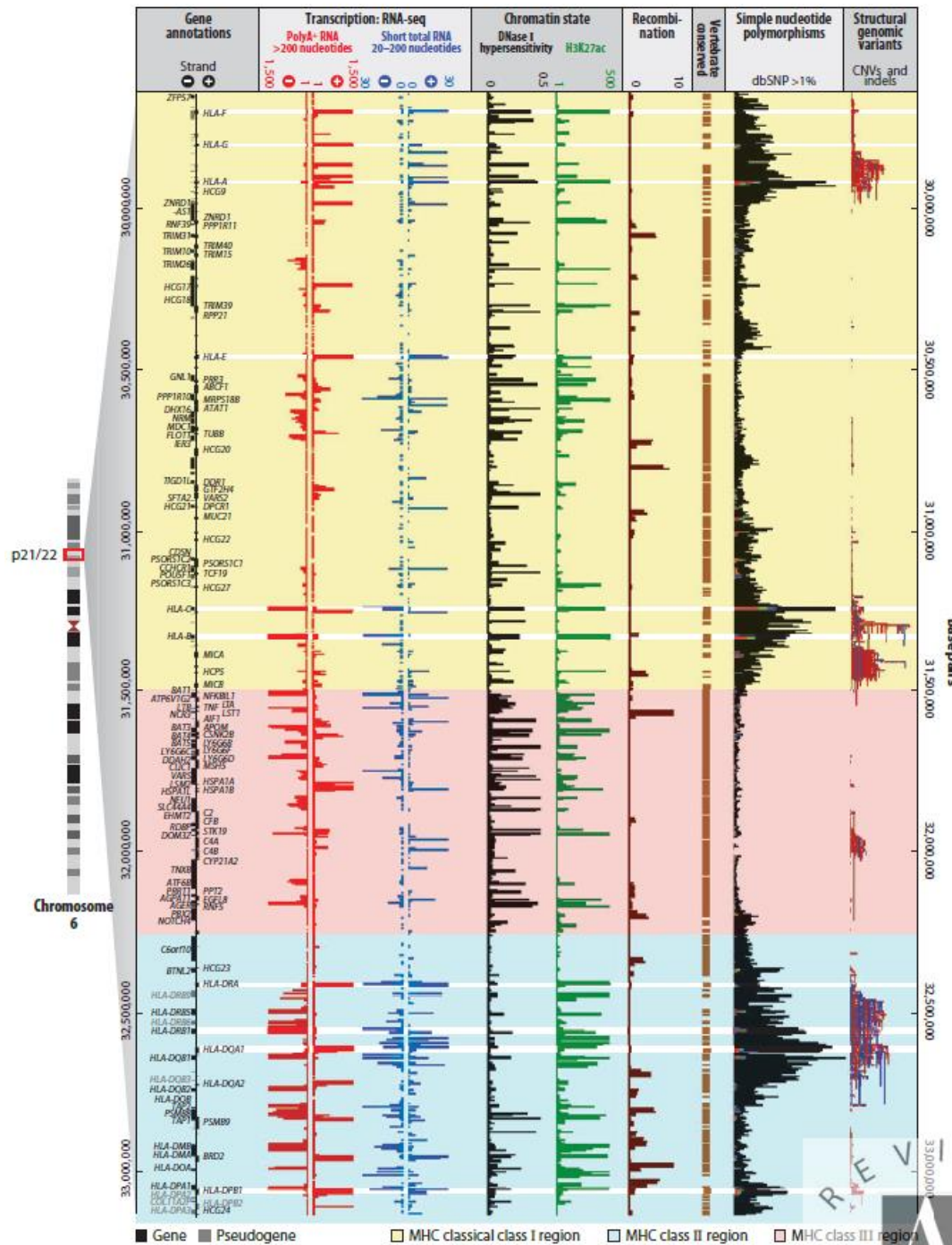


Major Histocompatibility Complex Genomics and Human Disease

John Trowsdale¹ and Julian C. Knight²

Annu. Rev. Genomics Hum. Genet. 2013.
14:16.1–16.23

HLA



Major Histocompatibility Complex Genomics and Human Disease

John Trowsdale¹ and Julian C. Knight²

Annu. Rev. Genomics Hum. Genet. 2013. 14:16.1-16.23

REVIEWS

Transplant Success & xHLA

- **HLA genes [HLA-A/B/C/F/G; HLA-DP/DQ/DR]**
- **non-HLA genes within the xHLA [MICA/MICB]**
- **Other genes outside xHLA**
 - ✓ **Cytokine Genes:** Variations in genes encoding cytokines, which are signalling molecules involved in immune responses, may influence the inflammatory environment and immune reactions after transplantation.
 - ✓ **Adhesion Molecule Genes:** Genes encoding adhesion molecules on cell surfaces may affect the adhesion and migration of immune cells, influencing the immune response to the transplanted tissue.
 - ✓ **Genes Related to Fibrosis and Tissue Repair:** Variations in genes involved in fibrosis and tissue repair processes may influence the development of fibrotic reactions in the transplanted organ.
 - ✓ **Immunosuppressive Medication Metabolism Genes:** Genes involved in the metabolism of immunosuppressive medications used post-transplantation can impact drug efficacy and patient outcomes.
 - ✓ **Innate Immune System Genes:** Genes associated with the innate immune system, such as toll-like receptors, may influence the early responses to transplantation.

Transplant Success & non-HLA

Findings

59 268 nsSNPs affecting a transmembrane or secreted protein were analysed. The median number of nsSNP mismatches in immune-accessible transmembrane and secreted proteins between donors and recipients was 1892 (IQR 1850–1936). The degree of nsSNP mismatch was independently associated with graft loss in a multivariable model adjusted for HLA eplet mismatch (*HLA-A*, *HLA-B*, *HLA-C*, *HLA-DP*, *HLA-DQ*, and *HLA-DR*). Each increase by a unit of one IQR had an HR of 1.68 (95% CI 1.17–2.41, $p=0.005$). 5-year death censored graft survival was 98% in the quartile with the lowest mismatch, 91% in the second quartile, 89% in the third quartile, and 82% in the highest quartile ($p=0.003$, log-rank test). Customised peptide arrays verified a donor-specific alloimmune response to genetically predicted mismatched epitopes.

Interpretation

Genetic mismatch of non-HLA haplotypes coding for transmembrane or secreted proteins is associated with an increased risk of functional graft loss independently of HLA incompatibility. As in HLA alloimmunity, donor-specific alloantibodies can be identified against genotype derived non-HLA epitopes.

Genome-wide nsSNP mismatch in transmembrane and secreted proteins was independent of HLA mismatch, including *HLA-DP* mismatch and independently associated with transplant outcome.

Contribution of non-HLA incompatibility between donor and recipient to kidney allograft survival: genome-wide analysis in a prospective cohort

Roman Reindl-Schwaighofer*, Andreas Heinzl*, Alexander Kainz, Jessica van Setten, Kira Jelencsics, Karin Hu, Bao-Li Loza, Michael Kammer, Georg Heinze, Petra Hruby, Alena Koňáříková, Ondrej Viklicky, Georg A Boehmig, Farsad Eskandary, Gottfried Fischer, Frans Claas, John C Tan, Tom J Albert, Jigar Patel, Brendan Keating, Rainer Oberbauer, for the iGeneTRAI consortium†

Transplant Success & non-HLA

	Hazard ratio (95% CI)	p value
nsSNP mismatch in transmembrane and secreted (per IQR)	1.68 (1.17-2.41)	0.005
nsSNP mismatch (without transmembrane or secreted, per IQR)	0.90 (0.63-1.28)	0.543
Genome-wide SNP mismatch (without nsSNP, per IQR)	1.02 (0.85-1.22)	0.858
HLA eplet mismatch (per IQR)	1.43 (1.01-2.02)	0.042

nsSNP mismatch in transmembrane and secreted proteins was independently associated with graft loss, and exhibited a similar risk per IQR increase as HLA eplet mismatch. SNP=single nucleotide polymorphism. nsSNP=non-synonymous single nucleotide polymorphism.

Table 2: Multivariable Cox proportional hazard model for death-censored kidney allograft loss

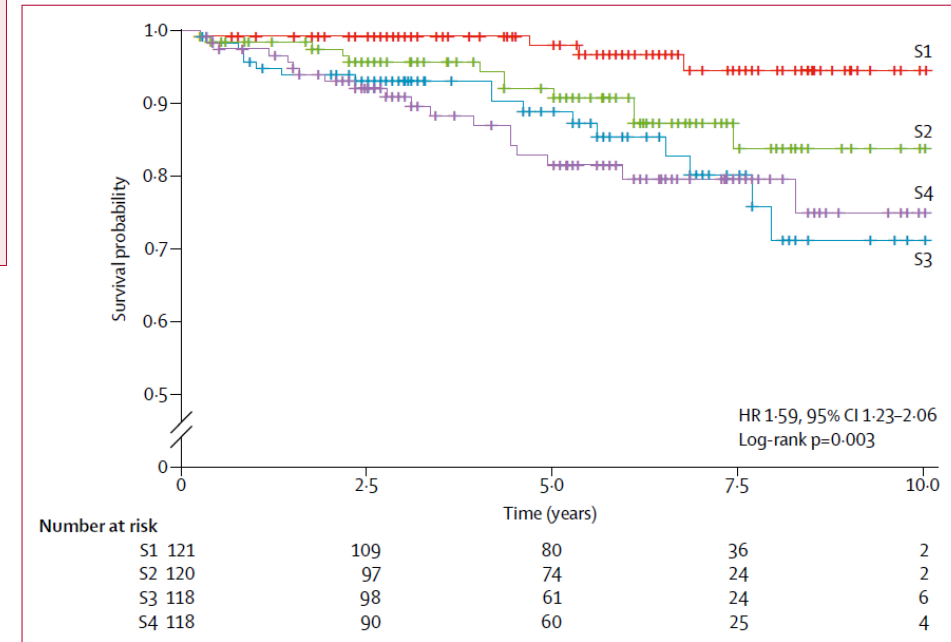


Figure 3: Kaplan-Meier plot of functional renal allograft survival, stratified by quartiles of nsSNP mismatch coding for transmembrane and secreted proteins

S1 denotes the lowest quartile and thus the lowest amount of mismatch, S4 the highest and thus the highest amount of mismatch. Differences between the survival curves were significant (log-rank p=0.003). nsSNP=non-synonymous single nucleotide polymorphism.

Contribution of non-HLA incompatibility between donor and recipient to kidney allograft survival: genome-wide analysis in a prospective cohort

Roman Reindl-Schwaighofer*, Andreas Heinzl*, Alexander Kainz, Jessica van Setten, Kira Jelencsics, Karin Hu, Bao-Li Loza, Michael Kammer, Georg Heinze, Petra Hruby, Alena Koňářiková, Ondrej Viklicky, Georg A Boehmig, Farsad Eskandary, Gottfried Fischer, Frans Claas, John C Tan, Tom J Albert, Jigar Patel, Brendan Keating, Rainer Oberbauer, for the iGeneTRAI consortium†

Transplant Success & HLA-F

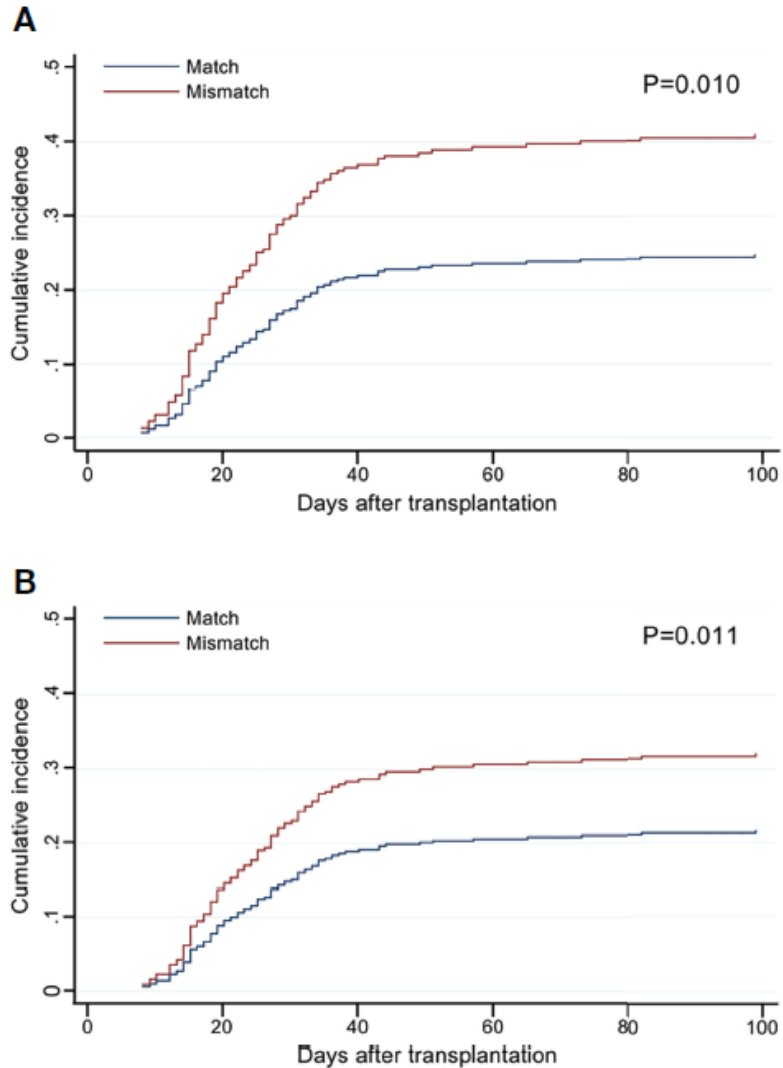


FIGURE 2 | Cumulative incidence of grade II–IV acute graft-versus-host disease (aGVHD) by the mismatch number of HLA-F-AS1 and HLA-DPB1 at the allele level in the GVH direction. (A, B) Cumulative incidence curves of HLA-F-AS1 and HLA-DPB1, respectively. Cumulative incidences at 100 days were HLA-F-AS1 match, 26% (95% CI, 21%–31%); HLA-F-AS1 mismatch, 42% (30%–55%); HLA-DPB1 match, 21% (15%–28%); and HLA-DPB1 mismatch, 34% (28%–41%).

Sequence Variations Within *HLA-G* and *HLA-F* Genomic Segments at the Human Leukocyte Antigen Telomeric End Associated With Acute Graft-Versus-Host Disease in Unrelated Bone Marrow Transplantation

Shingo Suzuki¹, Satoko Morishima², Makoto Murata³, Masafumi Tanaka¹, Atsuko Shigenari¹, Sayaka Ito¹, Uma Kanga⁴, Jerzy K. Kulski^{1,5}, Yasuo Morishima^{6,7} and Takashi Shiina^{1*}

Transplant Success & MICA/MICB

- **Role in Graft-versus-Host Disease (GVHD):** Polymorphisms in MICA and MICB genes have been associated with an increased risk of GVHD, a condition where transplanted immune cells attack the recipient's tissues. This is particularly relevant in the context of hematopoietic stem cell transplantation (HSCT).
- **NK Cell Recognition:** MICA and MICB molecules are ligands for NK cell receptors, such as NKG2D. Variations in MICA and MICB can affect the interaction between these ligands and receptors, influencing NK cell activation and responses to transplanted tissues.
- **Influence on Immune Response:** Polymorphisms in MICA and MICB may impact the immune response to transplanted organs or tissues, contributing to variations in graft acceptance or rejection.
- **Donor-Recipient Matching:** Matching MICA and MICB profiles between donors and recipients is an area of interest in transplantation. Some studies suggest that considering MICA and MICB polymorphisms in addition to traditional HLA matching may provide additional information for predicting transplant outcomes.

Transplant Success & MICA/MICB

All patients and donors were high-resolution HLA-typed and matched for 10/10 (n = 1379), 9/10 (n = 636), or 8/10 (n = 157) HLA alleles.

Mismatches at the MICA locus as well as MICA-129 increased with the number of HLA mismatches.

Adverse OS was observed in the **10/10 match** group if MICA-129 was mismatched (HR, 1.8; CI, 1.2 to 2.6; $P = 0.003$).; a significantly worse outcome for DFS (HR, 1.8; CI 1.3 to 2.5; $P = 0.001$).

Matching for the MICA-129 polymorphism is beneficial in unrelated hematopoietic stem cell transplantation

Daniel Fuerst,^{1,2} Christine Neuchel,^{1,2} Dietger Niederwieser,³ Donald Bunjes,⁴ Martin Gramatzki,⁵ Eva Wagner,⁶ Gerald Wulf,⁷ Bertram Glass,⁸ Michael Pfreundschuh,⁹ Hermann Einsele,¹⁰ Renate Arnold,¹¹ Gernot Stuhler,¹² Kerstin Schaefer-Eckart,¹³ Sebastian Freitag,¹⁴ Jochen Casper,¹⁵ Martin Kaufmann,¹⁶ Mohammed Wattad,¹⁷ Bernd Hertenstein,¹⁸ Stefan Klein,¹⁹ Mark Ringhoffer,²⁰ Daphne Mytilineos,² Chrysanthi Tsamadou,^{1,2} Cartheinz Mueller,^{21,22} Hubert Schrezenmeier,^{1,2} and Joannis Mytilineos^{1,2,22}

Transplant Success & MICA/MICB

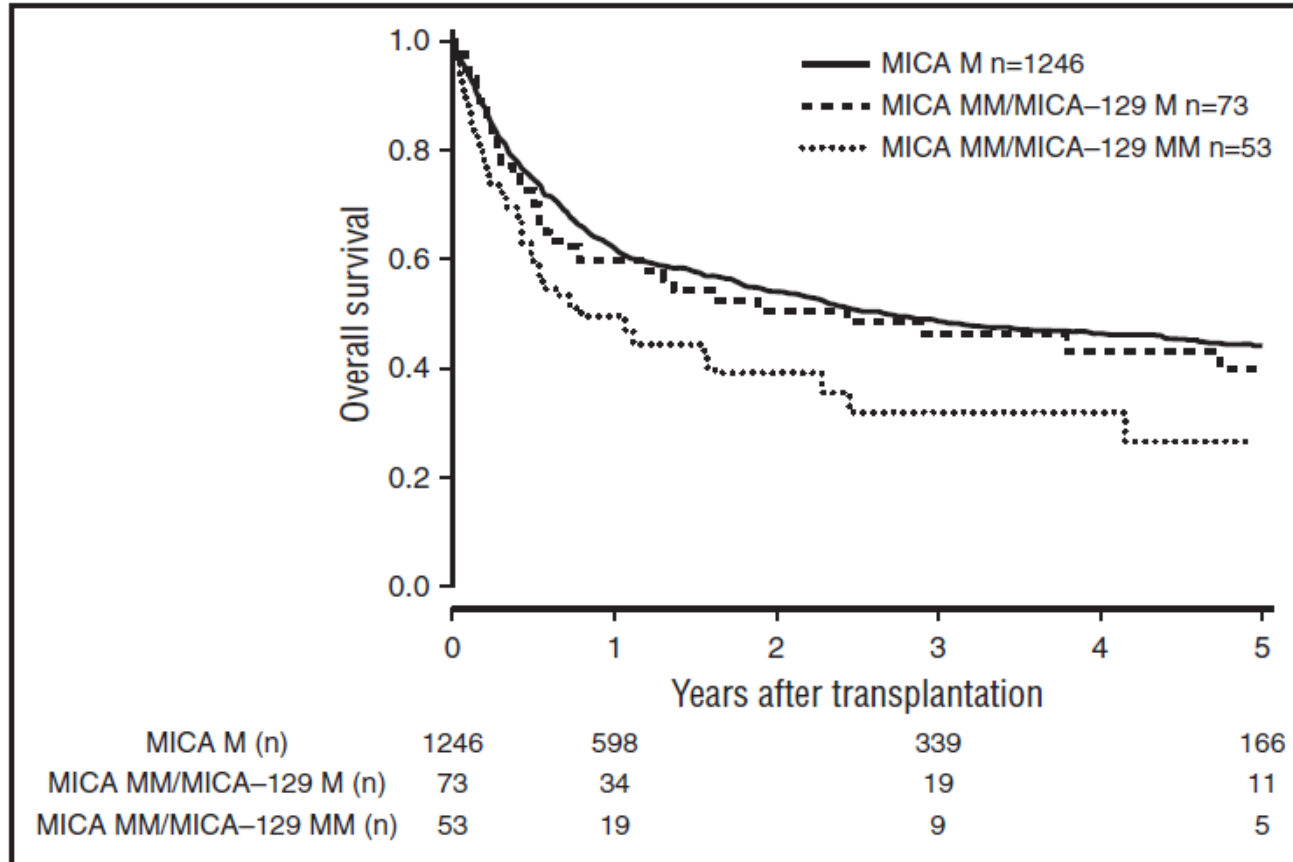


Figure 1. Overall survival of patients with 10/10 compatible donors transplanted with a MICA matched donor (solid black line), a MICA mismatched/MICA-129 matched donor (dashed line), and a MICA mismatched/MICA-129 mismatched donor (dotted line) ($P = 0.04$).

Matching for the MICA-129 polymorphism is beneficial in unrelated hematopoietic stem cell transplantation

Daniel Fuerst,^{1,2} Christine Neuchel,^{1,2} Dietger Niederwieser,³ Donald Bunjes,⁴ Martin Gramatzki,⁵ Eva Wagner,⁶ Gerald Wulf,⁷ Bertram Glass,⁸ Michael Pfreundschuh,⁹ Hermann Einsele,¹⁰ Renate Arnold,¹¹ Gernot Stuhler,¹² Kerstin Schaefer-Eckart,¹³ Sebastian Freitag,¹⁴ Jochen Casper,¹⁵ Martin Kaufmann,¹⁶ Mohammed Wattad,¹⁷ Bernd Hertenstein,¹⁸ Stefan Klein,¹⁹ Mark Ringhoffer,²⁰ Daphne Mytilineos,² Chrysanthi Tsamadou,^{1,2} Carlheinz Mueller,^{21,22} Hubert Schrezenmeier,^{1,2} and Joannis Mytilineos^{1,2,22}

Transplant Success & MICA/MICB

MICA mismatches were associated with decreased graft survival (HR, 2.12; 95% CI: 1.5 to 3.1; $P < 0.001$).

Both before and after transplantation anti-MICA donor-specific antibodies (DSA) were strongly associated with increased antibody-mediated rejection (ABMR) (HR, 3.8; 95% CI: 1.9 to 7.4; $P < 0.001$; HR, 9.9; 95% CI: 7.4 to 13.2; $P < 0.001$, respectively).

This effect was synergetic with that of anti-HLA DSA before and after transplantation (HR, 25.7; 95% CI: 3.3 to 199.4; $P = 0.002$; HR, 82.7; 95% CI: 33.7 to 203.0; $P < 0.001$, respectively).

De novo-developed anti-MICA DSA were the most harmful because they were also associated with reduced graft survival (HR, 1.3; 95% CI: 1.1 to 1.6; $P = 0.014$).

Finally, the damaging effect of anti-MICA DSA on graft survival was confirmed in an independent cohort of 168 patients with ABMR (HR, 1.7; 95% CI: 1.0 to 2.9; $P = 0.04$).

The MHC class I MICA gene is a histocompatibility antigen in kidney transplantation

Raphael Carapito^{1,2,3,4,5} , Ismail Aouadi^{1,2,3,5}, Martin Verniquet^{1,2,3,5}, Meiggie Untrau^{1,2,3,5}, Angélique Pichot^{1,2,3,5}, Thomas Beaudrey^{1,2,5,6}, Xavier Bassand^{1,2,5,6}, Sébastien Meyer^{1,2,3,5}, Loïc Faucher^{2,7}, Juliane Posson^{8,9}, Aurore Morlon^{2,10}, Irina Kotova^{2,10}, Florent Delbos^{2,11}, Alexandre Walencik^{2,11}, Alice Aarnink¹², Anne Kennel¹², Caroline Suberbielle^{2,13}, Jean-Luc Taupin^{2,13}, Benedict M. Matern¹⁴, Eric Spierings¹⁴, Nicolas Congy-Jolivet^{2,15,16}, Arnaud Essaydi¹⁷, Peggy Perrin^{1,2,5,6}, Antoine Blancher^{2,15,16}, Dominique Charron^{2,5,13}, Nezhir Cereb¹⁸, Myriam Maumy-Bertrand^{2,5,19}, Frédéric Bertrand^{2,5,19}, Valérie Garrigue^{2,20}, Vincent Pernin^{2,20}, Laurent Weekers²¹, Maarten Naesens²², Nassim Kamar^{2,23}, Christophe Legendre^{2,24}, Denis Glotz^{2,8,9}, Sophie Caillard^{1,2,5,6}, Marc Ladrrière²⁵, Magali Giral^{2,7}, Dany Anglicheau^{2,24,26}, Caner Süsal^{27,28} and Seiamak Bahram^{1,2,3,4,5} 

Transplant Success & MICA/MICB

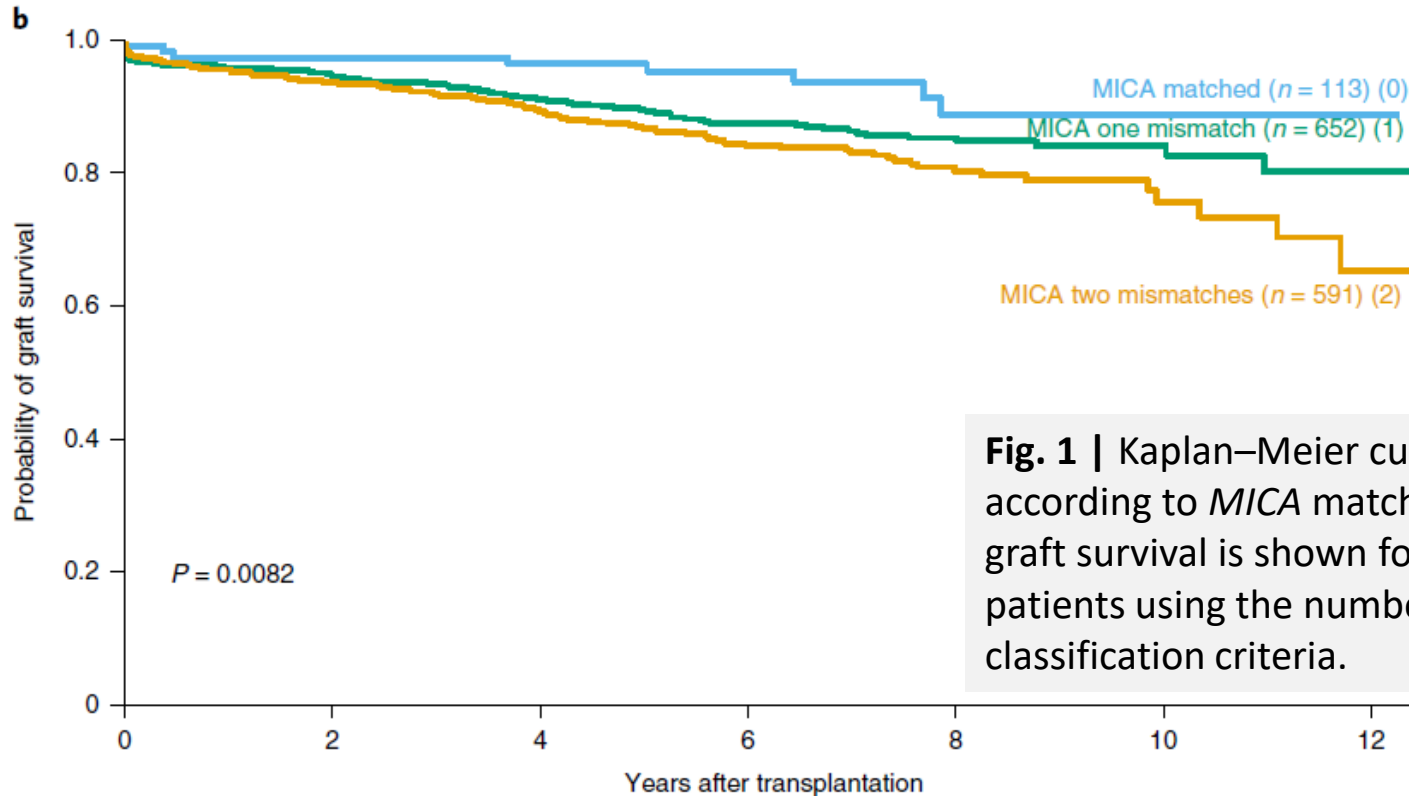


Fig. 1 | Kaplan–Meier curves for kidney graft survival according to *MICA* matching status. The probability of graft survival is shown for matched versus mismatched patients using the number of mismatches (**b**) as classification criteria.

The MHC class I *MICA* gene is a histocompatibility antigen in kidney transplantation

Raphael Carapito^{1,2,3,4,5}, Ismail Aouadi^{1,2,3,5}, Martin Verniquet^{1,2,3,5}, Meiggie Untrau^{1,2,3,5}, Angélique Pichot^{1,2,3,5}, Thomas Beaudrey^{1,2,5,6}, Xavier Bassand^{1,2,5,6}, Sébastien Meyer^{1,2,3,5}, Loïc Faucher^{2,7}, Juliane Posson^{8,9}, Aurore Morlon^{2,10}, Irina Kotova^{2,10}, Florent Delbos^{2,11}, Alexandre Walencik^{2,11}, Alice Aarnink¹², Anne Kennel¹², Caroline Suberbielle^{2,13}, Jean-Luc Taupin^{2,13}, Benedict M. Matern¹⁴, Eric Spierings¹⁴, Nicolas Congy-Jolivet^{2,15,16}, Arnaud Essaydi¹⁷, Peggy Perrin^{1,2,5,6}, Antoine Blancher^{2,15,16}, Dominique Charron^{2,5,13}, Nezh Cereb¹⁸, Myriam Maumy-Bertrand^{2,5,19}, Frédéric Bertrand^{2,5,19}, Valérie Garrigue^{2,20}, Vincent Pernin^{2,20}, Laurent Weekers²¹, Maarten Naesens²², Nassim Kamar^{2,23}, Christophe Legendre^{2,24}, Denis Glotz^{2,8,9}, Sophie Caillard^{1,2,5,6}, Marc Ladrrière²⁵, Magali Giral^{2,7}, Dany Anglicheau^{2,24,26}, Caner Süsal^{27,28} and Seiamak Bahram^{1,2,3,4,5}

Transplant Success & MICA/MICB

The lower graft survival can be explained by an increased rate of ABMR, which is independently associated with anti-MICA DSA.

The present data formally define MICA as a bona fide transplantation antigen in kidney organ transplants and provide the rationale for including *MICA* genotyping and immunization monitoring in the pre- and post-transplantation workup (but not *MICA* eplet mismatches instead of global *MICA* mismatches *).

[* Close to 400 *MICA* alleles have been reported to date]

The MHC class I *MICA* gene is a histocompatibility antigen in kidney transplantation

Raphael Carapito^{1,2,3,4,5} , Ismail Aouadi^{1,2,3,5}, Martin Verniquet^{1,2,3,5}, Meiggie Untrau^{1,2,3,5}, Angélique Pichot^{1,2,3,5}, Thomas Beaudrey^{1,2,5,6}, Xavier Bassand^{1,2,5,6}, Sébastien Meyer^{1,2,3,5}, Loïc Faucher^{2,7}, Juliane Posson^{8,9}, Aurore Morlon^{2,10}, Irina Kotova^{2,10}, Florent Delbos^{2,11}, Alexandre Walencik^{2,11}, Alice Aarnink¹², Anne Kennel ¹², Caroline Suberbielle^{2,13}, Jean-Luc Taupin^{2,13}, Benedict M. Matern ¹⁴, Eric Spierings ¹⁴, Nicolas Congy-Jolivet^{2,15,16}, Arnaud Essaydi¹⁷, Peggy Perrin^{1,2,5,6}, Antoine Blancher^{2,15,16}, Dominique Charron^{2,5,13}, Nezh Cereb¹⁸, Myriam Maumy-Bertrand^{2,5,19}, Frédéric Bertrand^{2,5,19}, Valérie Garrigue^{2,20}, Vincent Pernin^{2,20}, Laurent Weekers ²¹, Maarten Naesens ²², Nassim Kamar^{2,23}, Christophe Legendre^{2,24}, Denis Glotz^{2,8,9}, Sophie Caillard^{1,2,5,6}, Marc Ladrière²⁵, Magali Giral^{2,7}, Dany Anglicheau^{2,24,26}, Caner Süsal^{27,28} and Seiamak Bahram ^{1,2,3,4,5} 

Transplant Success & HLA-G

- **HLA-G contributes to immune tolerance (incl. fetal-maternal tolerance) and resisting rejection: Soluble HLA-G levels correlate with maternal-fetal tolerance**
- **3' UTR 14bp insertion/deletion polymorphism is associated with transplant rejection and soluble HLA-G levels**
- **HLA-G is thought to be involved in transplantation immune tolerance by protecting the organ from rejection**
- **In pathological situations, the molecule is observed in tumors and correlated to bad prognosis and is associated to autoimmune diseases and viral infection susceptibility, creating an unbalanced and pathologic environment**
- **HLA-G expression is also regulated by cytokines: IL-4 and IL-10 upregulates; IL-2 and IL-6 downregulates; IFN- γ and IL-10 maintains high expression**

Biological Characteristics of HLA-G and Its Role in Solid Organ Transplantation

Siqi Liu¹, Nicolaas A. Bos¹, Erik A. M. Verschuuren², Debbie van Baarle³ and Johanna Westra^{1}*

Transplant Success & HLA-G

Donor and recipient human leukocyte antigen-G polymorphisms modulate the risk of adverse immunologic events following lung transplantation

Peter Biddell¹, Jin Ao², Julietta Luzarte¹, Daniela Birznel¹, Anubhav Uthamanian¹, Rashied Ghany¹, Diego Delgado¹, Vivek Rao³, Sher Keshavjee¹, Teresa Martino¹, Iusti Tikkanen¹

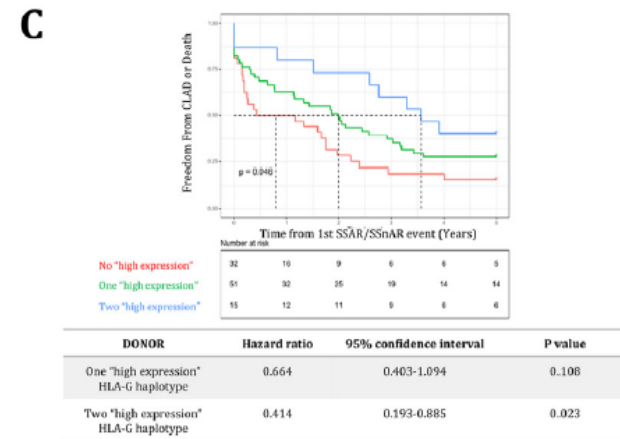
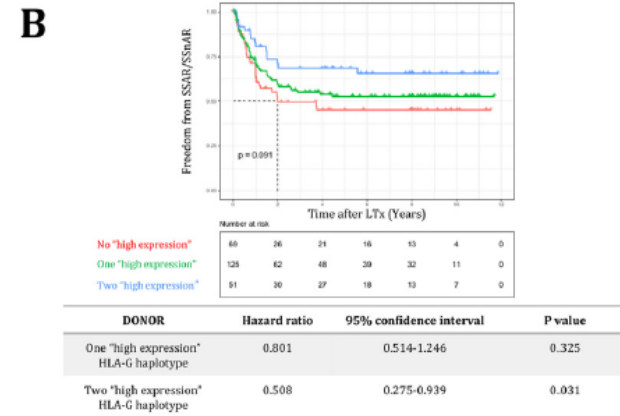
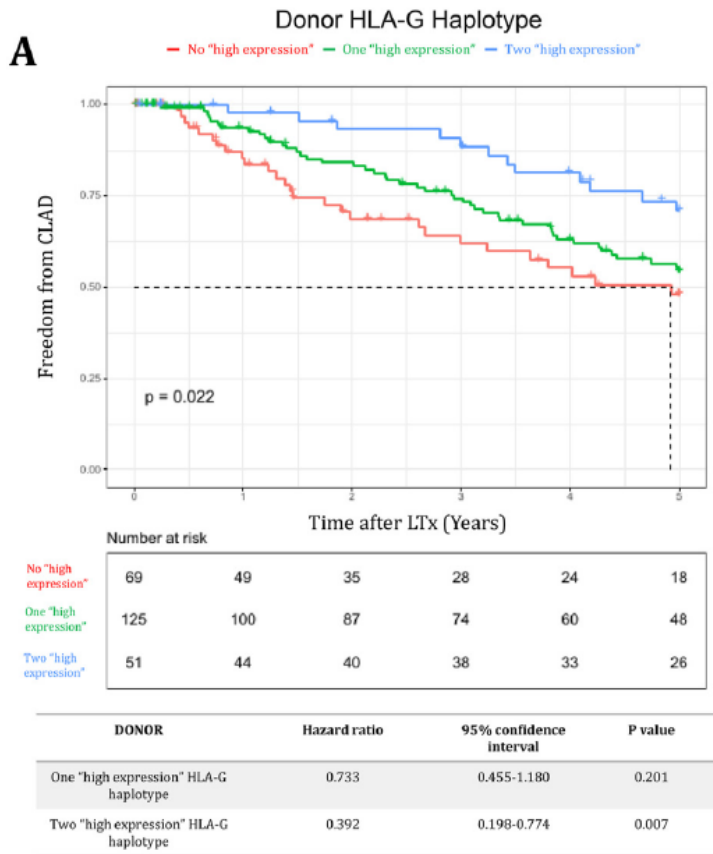


Figure 1. HLA-G haplotypes were characterized as exhibiting low or high HLA-G expression based on the reported effects of each haplotype or by extrapolating the effects of individual SNPs on overall haplotype function. With this characterization, we performed Kaplan–Meier analysis to assess the effect of donor HLA-G haplotype on (A) the time to CLAD (censored at 5 years post-LTx), (B) the time to first SSAR/SSnAR, and (C) the time from first SSAR/SSnAR to either CLAD or death (analysis censored at 5 years post-SSAR/SSnAR). Below each graph, we report the numbers at risk and univariable Cox proportional hazards ratios. The comparator group is where both donor haplotypes exhibit low HLA-G expression. CLAD, chronic lung allograft dysfunction; HLA-G, human leukocyte antigen-G; LTx, lung transplantation; SNP, single nucleotide polymorphisms; SSAR, spirometrically significant acute rejection event; SSnAR, spirometrically significant nonacute rejection event.

Conclusions

The HLA complex contains disproportional number of genes and polymorphisms

The extra-ordinary features of the HLA complex will certainly continue to create surprises in human genetics

Full (10/10) HLA antigen matching is a desirable feature for transplant success, but there is still room for further improvement

Some non-HLA polymorphisms within and outside the HLA complex may contribute to variable outcomes even in 10/10-matched transplant recipients

There are calls for MICA to be considered as a transplant antigen

The involvement of HLA-G via induction of immune tolerance in transplant outcomes (as in pregnancy) promises interesting prospects

Thank You



HİTİD **MEMORIAL**

**HLA IMMUNOGENETICS AND TRANSPLANTATION
IMMUNOLOGY ASSOCIATION**
2nd TRANSPLANTATION IMMUNOLOGY COURSE
HOSTED BY MEMORIAL ŞİŞLİ HOSPITAL
29th-30th MARCH, 2024

